Optics and Lasers in Engineering 54 (2014) 232–235

Contents lists available at ScienceDirect

Optics and Lasers in Engineering

journal homepage: www.elsevier.com/locate/optlaseng

Heterodyne moiré interferometry for measuring corneal surface profile

Wei-Yao Chang [a], Kun-Huang Chen [b,*], Der-Chin Chen [b], Jung-Kai Tseng [c], Shyan-Tarng Chen [c], Han-Ying Sun [c], Jing-Heng Chen [d], Ken Y. Hsu [a]

[a] Department of Photonics and Institute of Electro-Optical Engineering, National Chiao Tung University, 1001 Ta-Hsueh Road, Hsinchu 30050, Taiwan, ROC
[b] Department of Electrical Engineering, Feng Chia University, No. 100, Wen Hwa Road, Taichung 40724, Taiwan, ROC
[c] School of Optometry, Chung Shan Medical University, No. 110, Section 1, Jianguo N. Road, Taichung City 40201, Taiwan, ROC
[d] Department of Photonics, Feng Chia University, No. 100, Wen Hwa Road, Taichung 40724, Taiwan, ROC

ARTICLE INFO

Article history:
Received 9 May 2013
Received in revised form
15 July 2013
Accepted 17 July 2013
Available online 8 August 2013

Keywords:
Corneal surface profile
Heterodyne interferometry
Projection moiré
Talbot effect

ABSTRACT

This study proposes an accurate method for reconstructing the corneal surface profile. By applying a constant velocity to the projection grating along the grating plane, a series of sampling points of the sinusoidal wave, which behaves in the manner of heterodyne interferometric signals, can be recorded using a CMOS camera. The phase distribution of the moiré fringes can then be obtained using the IEEE 1241 least-square sine fitting algorithm and two-dimensional (2D) phase unwrapping. Finally, the corneal surface profile can be reconstructed by substituting the phase distribution into a specially derived equation. To validate the proposed method, the corneal surface of a pig eyeball was measured. The measurement resolution was approximately 3.5 μm. Because of the introduction of the Talbot effect, the projection moiré method, and heterodyne interferometry, this approach provides the advantages of a simple optical setup, ease of operation, high stability, and high resolution.

1. Introduction

The refractive power of the cornea is more than two-thirds of the total refractive power of the human eye; therefore, a slight variation of the corneal surface can drastically affect normal human vision. Accurate reconstruction of the corneal surface profile can thus provide essential information for vision diagnosis. Various optical methods have been proposed for this purpose. Placido-disc topography [1–3], which involves analyzing reflected images and using the spherical approximation algorithm, is the most common technique used for reconstructing the corneal surface profile. However, this approach can incur height estimation errors at the same curvature, and the test edge yields a lower-quality measurement result. Other methods, such as the slit scanning method [4,5] and the Scheimpflug imaging method [6,7], have also been proposed. These methods can be used to acquire information on the corneal thickness and the profiles of the anterior and posterior corneal surfaces. However, during the measurement process, fringe projection scanning or rotating camera scanning is required, which renders the process time-consuming and may generate fixed-position errors. Although the described methods demonstrate the benefits of structural simplicity and ease of operation, the accuracy of measurement and resolution tend to be limited by fluctuations in the light intensity of the test. Therefore, this study proposes a simple approach for reconstructing the corneal surface profile based on the Talbot effect, the projection moiré method, and heterodyne interferometry. A linear grating is obliquely illuminated by an expanding collimated light, and a self-image of this grating can be generated and projected onto the corneal surface. The deformed grating fringes are imaged onto the second grating to form the moiré fringes. If the first grating is moved at a constant velocity along the grating plane, then a series of sampling points of the sinusoidal wave, which behaves in the manner of heterodyne interferometric signals, can be recorded using a CMOS camera. The phase distribution of the corneal surface can then be obtained using the IEEE 1241 least-square sine fitting algorithm and two-dimensional (2D) phase unwrapping. Finally, the corneal surface profile can be reconstructed by substituting the phase distribution into a special derived equation. This method demonstrates the benefits of the projection moiré method, the Talbot effect, and heterodyne interferometry, including simple optical setup, ease of operation, high stability, and high resolution.

2. Principle

Fig. 1 shows the optical configuration of the proposed method. For convenience, the z-axis is assigned as the observation axis of the CMOS camera, and the y-axis is set perpendicular to the paper

* Corresponding author. Tel.: +886 4 2451 7250x3831; fax: +886 4 2451 6842.
E-mail address: chenkh@fcu.edu.tw (K.-H. Chen).

0143-8166/$ - see front matter © 2013 Elsevier Ltd. All rights reserved.
http://dx.doi.org/10.1016/j.optlaseng.2013.07.013

plane. A laser light at wavelength λ passes through a beam expander to form an expanded and collimated light, and then impinges on a linear grating G_1 at an incident angle of α to the normal of the grating plane. The self-images of grating G_1 can be generated at the Talbot distances Z_T and can be expressed as [8]

$$Z_T = \frac{mp^2}{\lambda}\cos^3(\alpha), \quad m = 1,\ 2,\ 3\ldots \tag{1}$$

where p is the pitch of the grating G_1. After arranging the test sample on the first Talbot distance ($m=1$) of grating G_1, the grating fringes are self-imaged on the sample and deformed by the height distribution. The deformed grating fringes can be expressed as

$$I_1(x,y) = \frac{1}{2}\left\{1 + \cos\left[\frac{2\pi}{p}x + \theta(x,y) + \phi_1\right]\right\}, \tag{2}$$

where ϕ_1 is the initial phase of grating G_1, and $\theta(x, y)$ denotes the phase of the height distribution on the sample, expressed as

$$\theta(x,y) = \frac{2\pi}{p}H(x,y)\tan\ \alpha. \tag{3}$$

In Eq. (3), $H(x, y)$ is the height distribution on the sample. Eq. (3) can be rewritten as

$$H(x,y) = \frac{p}{2\pi\tan\ \alpha}\theta(x,y). \tag{4}$$

According to Eq. (4), $\theta(x, y)$ is a function of $H(x, y)$; therefore, the height distribution of the sample $H(x, y)$ can be estimated by accurately measuring the phase $\theta(x, y)$.

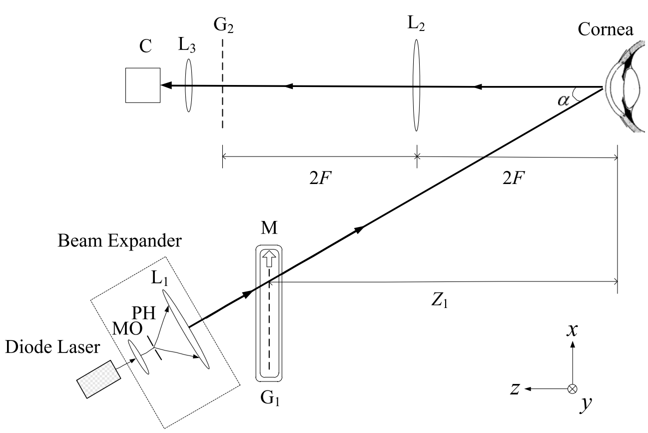

Fig. 1. Optical configuration. MO: microscopic objective; PH: pinhole; L_1: collimating lens; L_2: imaging lens; L_3: camera lens; G_1 and G_2: linear grating; M: motorized translation stage; Z_1: first Talbot distance; α: projection angle; F: focal length of imaging lens; C: CMOS camera.

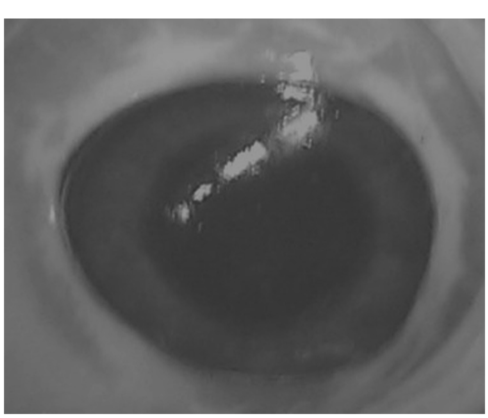

Fig. 2. The tested sample of the pig eyeball.

In the subsequent step, the deformed fringes are imaged at 1 × magnification on the grating G_2 of a pitch p to form the moiré fringes and are captured using a camera lens L_3 on the CMOS camera C. The captured fringes can be expressed as

$$\begin{aligned} I_2(x,y) &= I_1(x,y) \times T \\ &= \frac{1}{2}\left\{1 + \cos\left[\frac{2\pi}{p}x + \theta(x,y) + \phi_1\right]\right\} \times \frac{1}{2}\left[1 + \cos\left(\frac{2\pi}{p}x + \phi_2\right)\right], \end{aligned} \tag{5}$$

where T is the transmission of the grating G_2, and ϕ_2 is the initial phase of grating G_2. Eq. (5) can then be expanded as

$$\begin{aligned} I_2(x,y) = \frac{1}{4}\Bigg\{&1 + \cos\left[\frac{2\pi}{p}x + \theta(x,y) + \phi_1\right] + \cos\left(\frac{2\pi}{p}x + \phi_2\right) \\ &+ \frac{1}{2}\cos\left[\frac{4\pi}{p}x + \theta(x,y) + \phi_1 + \phi_2\right] + \frac{1}{2}\cos\left[\theta(x,y) + \phi_1 - \phi_2\right]\Bigg\}. \end{aligned} \tag{6}$$

In Eq. (6), the second, third, and fourth terms are the high-order harmonics, and the final term is a moiré fringe. The moiré fringes

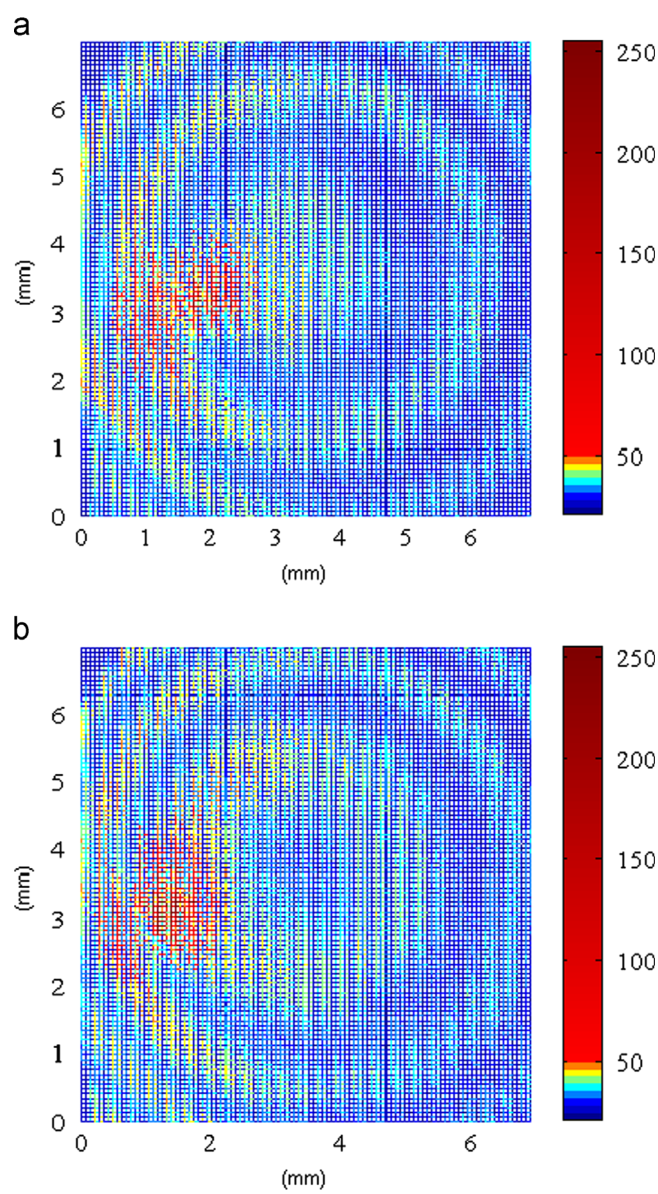

Fig. 3. Moiré fringes recorded by CMOS camera. (a and b) Moiré fringes at 0 s and 7/15 s.

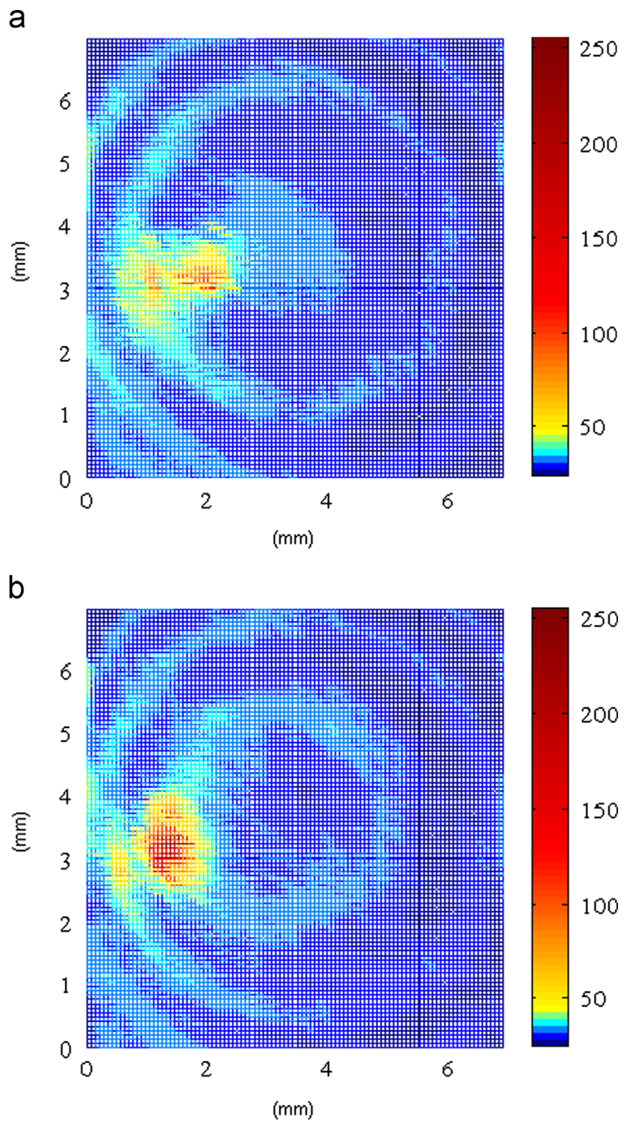

Fig. 4. (a and b) The results from applying the 2D median filter to filter Fig. 3(a) and (b).

can be extracted by filtering the high-order harmonics, and can be expressed as

$$I(x,y)=I_0(x,y)+\gamma(x,y)\cos[\theta(x,y)+\eta], \tag{7}$$

where $\gamma(x, y)$ is the visibility of the signal, and $\eta=\phi_1-\phi_2$ is the relative phase induced by the relative displacement between two gratings. When a motorized translation stage M moves the grating G_1 along the grating plane at a constant velocity v, the time-varying phase can be induced and expressed as

$$\eta=\frac{2\pi vt}{p}=2\pi f_h t, \tag{8}$$

where f_h is the heterodyne frequency resulting from the time-varying phase. Each pixel of the CMOS camera records a series of sampling points of the sinusoidal waves. These sinusoidal waves behave in the manner of heterodyne interferometric signals. Therefore, the light intensity at the CMOS camera C can be expressed as

$$I(x,y)=I_0(x,y)+\gamma(x,y)\cos[2\pi f_h t+\theta(x,y)], \tag{9}$$

To obtain $\theta(x, y)$, Eq. (9) can be rewritten as

$$I(x,y)=A\cos(2\pi f_h t)+B\sin(2\pi f_h t)+C, \tag{10}$$

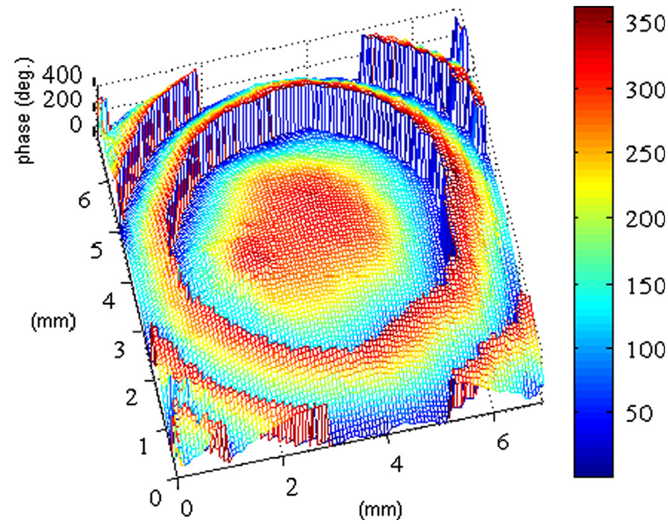

Fig. 5. Wrapped phase distribution of the corneal surface of the pig cornea.

where A, B, and C are real numbers, and the relationship between A, B, and $\theta(x, y)$ can be shown as

$$\theta(x,y)=\tan^{-1}\left(\frac{-B}{A}\right). \tag{11}$$

The terms A and B can be estimated using the least-squares sine wave fitting algorithm. Substituting A and B into Eq. (11) yields the corresponding phase $\theta(x, y)$ of the pixel. The phase distribution of the sample can be obtained by applying this procedure to each pixel and using 2D phase unwrapping. The sample surface profile can then be reconstructed using Eq. (4).

3. Experimental results and discussions

The proposed method was validated by using it to measure the corneal surface of a pig eyeball, as shown in Fig. 2. The experiment setup included a diode laser at a wavelength of 473 nm, two linear gratings at a pitch of 0.2822 mm, an imaging lens with a focal length of 200 mm, a motorized translation stage (Sigma Koki/SGSP (MS)26-100) with 0.05 μm resolution to produce a heterodyne frequency $f_h=2$ Hz ($v=0.5644$ mm/s), and a CMOS camera (Basler/A504k) with an 8-bit gray level and 1280 × 1024 image resolution. For convenience, the projection angle was 30°, the frame rate of the camera $f_s=30$ fps, the exposure time $\Delta t=0.033$ s, and the total recording time $\Delta T=1$ s to record the interferometric signals at different time points. To improve the visibility of the projected grating fringes, fluorescein was used to stain the corneal surface. The experimental results are displayed in Figs. 3–6. Fig. 3(a) and (b) shows the moiré fringes recorded by the camera at 0 s and 7/15 s, respectively. Fig. 4(a) and (b) shows the results obtained after applying the 2D median filter to filter Fig. 3 (a) and (b), respectively. Fig. 5 displays the phase distribution estimated using the least-squares sine fitting algorithm. Using 2D phase unwrapping and Eq. (4), the corneal surface profile can be reconstructed, as shown in Fig. 6. To prove the feasibility of proposed method, the identical vertical principle meridian of the corneal surface was extracted from the experimental results shown in Fig. 6 and the side view of the cornea shown in Fig. 7. The side view of the corneal sample in x–z plane was captured using the CMOS camera with the same magnification of the camera lens L_3. The vertical principle meridian of the corneal surface could be drawn along the boundary where the light intensity decreases substantially from the black part to the gray

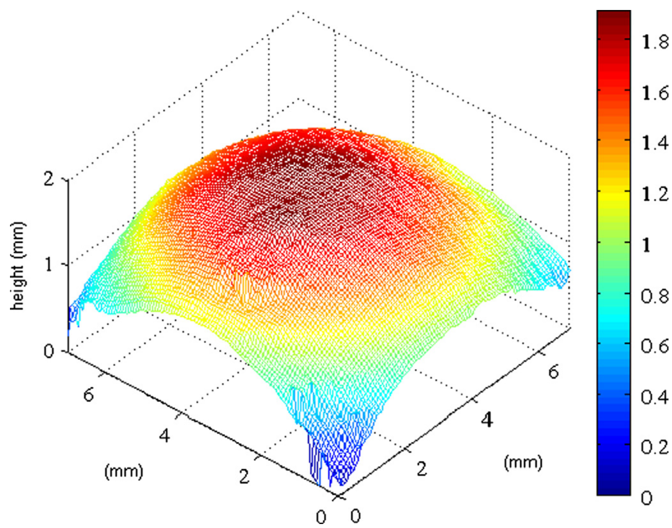

Fig. 6. Reconstructed surface profile of the pig cornea.

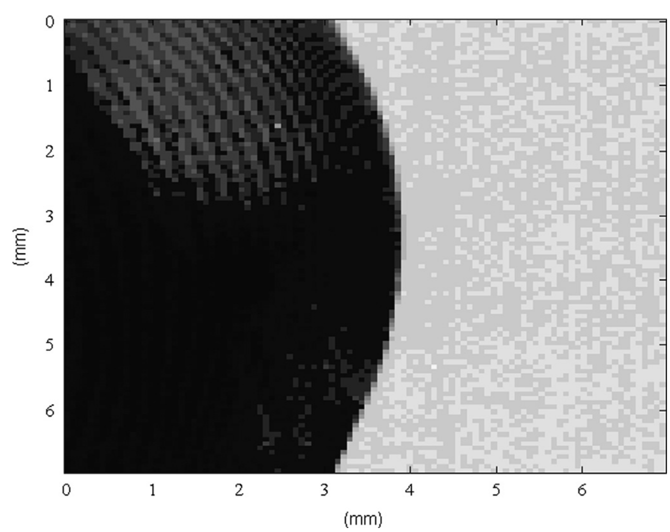

Fig. 7. Side view of cornea.

part, and was used to be the reference data. Fig. 8 shows the vertical principle meridians extracted from the experimental data and the reference data. The experimental data exhibit the same height trend as that of the reference data and, consequently, can prove the feasibility of proposed method, despite the reference data providing an unsmooth curve because of considerably lower resolution.

According to Eq. (4), the measurement height error ΔH can be expressed as

$$\Delta H = \left|\frac{\partial H}{\partial p}\Delta p\right| + \left|\frac{\partial H}{\partial \alpha}\Delta\alpha\right| + \left|\frac{\partial H}{\partial \theta}\Delta\theta\right|. \quad (12)$$

where Δp is the grating pitch error, $\Delta\alpha$ is the projection angle error, and $\Delta\theta$ is the phase error. The grating pitch error Δp is caused by grating fabrication. The gratings are fabricated by applying chromium plating onto a glass substrate by using a mask laser writer. The grating pitch error Δp is approximately 0.1 μm. The projection angle error $\Delta\alpha$ is introduced according to the axis alignment error and the resolution of the rotary stage for

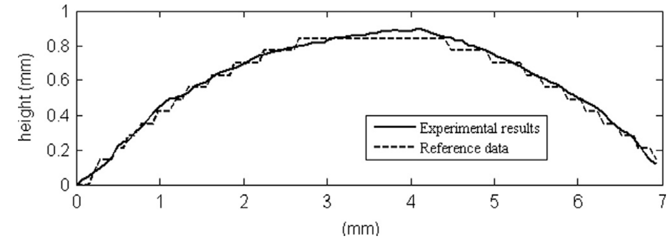

Fig. 8. Vertical principle meridians of cornea surface from experimental results and reference data.

alignment. Considering that the axis alignment error in the experiment is 0.05°, and the resolution of the rotary stage is 10′, the projection angle error $\Delta\alpha$ can be estimated at approximately 0.22°. The phase error $\Delta\theta$ is introduced according to the sampling error [9]. Considering that the visibility of the moiré fringes is 0.3, the stability of light intensity resulted from the stability of the light source and the vibration of the grating is 1%, and according to heterodyne interferometry, the phase error $\Delta\theta$ can be estimated at approximately 0.9°. By substituting the experimental conditions, Δp, $\Delta\alpha$, and $\Delta\theta$ into Eq. (12), the measurement height error ΔH is approximately 3.5 μm. This error analysis indicates that the proposed technique yields high accuracy and high resolution.

4. Conclusion

This study proposes a simple method for reconstructing the corneal surface profile. The proposed method was validated by using it to measure the corneal surface of a pig eyeball. The measurement resolution was approximately 3.5 μm. The proposed approach demonstrates the benefits of the projection moiré method, the Talbot effect, and heterodyne interferometry, including simple optical setup, ease of operation, high stability, and high resolution.

Acknowledgments

The authors would like to thank the Cooperation Plan Case of the Chung Shan Medical University and Feng Chia University, Taiwan, and the National Science Council of the Republic of China, Taiwan for financially supporting this research under Contracts no. 12G27303, and NSC 101-2221-E-009-112-MY3.

References

[1] Corbett MC, Rosen ES, O'Brart DP. Corneal topography: principles and applications. London: BMJ Books; chapter 1–3.
[2] Jongsma FHM, Brabander Jd, Hendrikse F. Review and classification of corneal topographers. Lasers Med Sci 1999;14:2–19.
[3] Massig JH, Lingelbach E, Lingelbach B. Videokeratoscope for accurate and detailed measurement of the cornea surface. Appl Opt 2005;44(12):2281–7.
[4] Liu Z, Huang AJ, Pflugfelder SC. Evaluation of corneal thickness and topography in normal eyes using the Orbscan corneal topography system. Br J Ophthalmol 1999;83:774–8.
[5] Cairns G, Collins A, McGhee CN. A corneal model for slit-scanning elevation topography. Ophthalmic Physiol Opt 2003;3(3):193–204.
[6] Swartz T, Marten L, Wang M. Measuring the cornea: the latest developments in corneal topography. Curr Opin Ophthalmol 2007;18(4):325–33.
[7] Oliveira CM, Ribeiro C, Franco S. Corneal imaging with slit-scanning and Scheimpflug imaging techniques. Clin Exp Optom 2011;94(1):33–42.
[8] Testorfa M, Jashnsa J, Khilob NA, Goncharenkob AM. Talbot effect for oblique angle of light propagation. Opt Commun 1996;129(3–4):167–72.
[9] Jian ZC, Chen YL, Hsieh HC, Hsieh PJ, Su DC. Optimal condition for full-field heterodyne interferometry. Opt Eng 2007;46(11):115604-1–8.